Analysis of the Rician *K*-Factor in a Typical Millimeter-Wave Office Scenario

Lorenzo Rubio, *Senior Member, IEEE*, Vicent M. Rodrigo Peñarrocha, Juan Reig, *Senior Member, IEEE*, Herman Fernández, Jesús R. Pérez, Rafael P. Torres, and Luis Valle

***Abstract*—In this letter, the *K*-factor is estimated in a typical office scenario based on wideband channel measurements carried out at millimeter-wave (mmWave) frequencies, covering the 25–40 GHz spectrum, in both line-of-sight (LOS) and obstructed-LOS (OLOS) propagation conditions. The *K*-factor is estimated from the method of moments, applied directly over the frequency samples of the measured complex channel transfer function, and from the power delay profile-based method. Although both methods provide similar results, the method of moments is more appropriate from a practical point of view, especially in OLOS and non-LOS (NLOS) conditions, where the correct identification of dominant components can be difficult. The results are particularized to the potential 26, 28, 33, and 38 GHz frequency bands for the design and deployment of the future wireless networks at mmWave frequencies. The mean value of the *K*-factor ranges from −1.87 to 1.27 dB for the LOS condition, and from −3.79 to −2.31 dB for the OLOS condition.**

***Index Terms*—Fading channels, millimeter-wave (mmWave), Rice distribution, small-scale fading, *K*-factor.**

I. Introduction

In WIRELESS communications, the multipath contributions (MPCs) can arrive at the receiver position through different reflection, diffraction, and scattering processes [1]. The superposition of all MPCs produces temporal dispersion, equivalent to frequency selectivity [1], [2]. On the other hand, the time variability of the propagation channel due to the Doppler effect produces temporal and spatial selectivity. The Rician *K*-factor is a parameter commonly used to describe the small-scale fading in time, space, or frequency of the received signal envelope.

The Rician *K*-factor is defined as the power ratio of the dominant component to the stochastic MPCs [1]. Thus, when the dominant component is attenuated compared to the rest of MPCs, the *K*-factor decreases. In the limit, when the dominant component disappears the *K*-factor reaches a value of 0 ($-\infty$ dB), corresponding to the case of maximum selectivity in the channel, and the received signal envelope fluctuations can be described by the well-known Rayleigh distribution [1]. Therefore, the knowledge of the *K*-factor has an important implication in the design of transmission and reception techniques oriented to mitigate the small-scale fading, such as modulation and adaptive coding techniques [3], diversity schemes [4], [5], optimal configuration of orthogonal frequency division multiple access techniques (OFDMA) [6], and system complexity in massive multiple-input–multiple-output (MIMO) systems [7], [8], among others.

In literature, different estimators of the *K*-factor have been proposed for time-varying narrowband channels, such as the method of moments [9], [10], and the maximum-likelihood (ML) method [11], which work with temporal samples of the received signal envelope. However, modern wireless communications operate over large bandwidths, as it is the case of fifth- and sixth-generation (5G and 6G) systems, where bandwidths of several megahertz are considered. In narrowband systems, it is relatively easy to carry out experimental measurements to analyze the time-varying behavior of the propagation channel. On the contrary, in wideband systems, and in particular at millimeterwave (mmWave) frequencies, to perform channel measurements oriented to analyze small-scale fading is very difficult due to high cable losses and mobility effects. In [12], under the assumption of wide-sense stationary uncorrelated scattering (WSSUS), the authors demonstrated that it is possible to estimate the *K*-factor in wideband channels from a single-snapshot measurement. This facilitates the analysis of temporal variability at mmWave frequencies based on experimental measurements conducted with traditional channel sounders that require stationary conditions, such as those based on vector network analyzers (VNAs).

In this letter, we estimate the *K*-factor from wideband channel measurements at mmWave frequencies conducted in a typical office environment using a frequency channel sounder, covering the 25–40 GHz spectrum, in both line-of-sight (LOS) and obstructed-LOS (OLOS) propagation conditions. Two methods have been applied: 1) the method of moments working directly with the frequency samples of the measured channel transfer function (CTF), and 2) a method based on the power delay profile (PDP) derived from the channel impulse response (CIR). The

Manuscript received 10 November 2023; revised 5 December 2023 and 3 January 2024; accepted 30 January 2024. Date of publication 6 February 2024; date of current version 7 May 2024. This work was supported by the MCIN/AEI/10.13039/501100011033/ through the I+D+i Projects under Grant PID2020-119173RB-C21 and Grant PID2020-119173RB-C22. *(Corresponding author: Lorenzo Rubio.)*

Lorenzo Rubio, Vicent M. Rodrigo Peñarrocha, and Juan Reig are with the Antennas and Propagation Lab, iTEAM Research Institute, Universitat Politècnica de València, 46022 Valencia, Spain (e-mail: lrubio@dcom.upv.es; vrodrigo@dcom.upv.es; jreigp@dcom.upv.es).

Herman Fernández is with the Escuela de Ingeniería Electrónica, Universidad Pedagógica y Tecnológica de Colombia, Sogamoso 152211, Colombia (e-mail: herman.fernandez@uptc.edu.co).

Jesús R. Pérez, Rafael P. Torres, and Luis Valle are with the Departamento de Ingeniería de Comunicaciones, Universidad de Cantabria, 39005 Santander, Spain (e-mail: jesusramon.perez@unican.es; rafael.torres@unican.es; luis.valle@unican.es).

Digital Object Identifier 10.1109/LAWP.2024.3362408

results of both methods are compared and discussed. The results have been particularized to the potential 26, 28, 33, and 38 GHz frequency bands to deploy the future wireless networks [13].

The rest of this letter is organized as follows. Section II describes the channel measurements. Section III indicates how the *K*-factor can be estimated from channel measurements. Results are presented and discussed in Section IV. Finally, Section V concludes this letter.

II. Channel Measurements

The channel measurements were conducted in a typical office environment of a modern construction building, where there is different furniture, such as chairs, work desks with computer screens and cabinets, among others. The dimensions of the propagation environment are 9.68×6.93 m^2, and the ceiling is at a height of 2.63 m.

The channel measurements were collected using a frequency channel sounder implemented through the Keysight N5227 A VNA. The $s_{21}(f)$ parameter, equivalent to the CTF, was measured directly from 25 to 40 GHz, with 8192 frequency samples, resulting in a frequency resolution of about 1.83 MHz. This frequency resolution corresponds to a maximum observable distance equal to 164 m, higher than the dimensions of the propagation environment. Ultrawideband omnidirectional antennas, with linear polarization, were used at the transmitter (Tx) and receiver (Rx) sides. In order to avoid the high losses introduced by cables, a radio-over-fiber link was used to connect the Tx subsystem to the output port of the VNA.

The Rx antenna was placed on a 2-D positioning system, implementing a 12×12 virtual uniform rectangular array (URA), with a separation between elements equal to 3.04 mm ($\approx \lambda/4$ at 25 GHz). The Tx antenna was placed at different positions in the room, and the Rx subsystem remained in the same position near one of the walls, emulating the position of a base station serving the user terminals (UTs) inside the room. The Rx antenna was placed at a height of 1.62 m, and the Tx antenna was positioned at a height of 0.90 m above the floor level and close to the desks imitating a UT, e.g., a tablet or a laptop. The channel measurements were conducted under both LOS and OLOS propagation conditions. In OLOS condition, the direct component was blocked by the computer screens. Fig. 1 shows a schematic of the propagation environment, where the location of the Rx antenna and the different positions of the Tx antenna are depicted. The Tx–Rx distance ranged from 2.70 to 8.40 m.

The bandwidth of the intermediate frequency filter of the VNA was set to 100 Hz, and a response calibration of all channel sounder elements was performed, before and during the measurements process. The channel measurements were carried out at night and during weekend, without the presence of people. More details about the channel sounder, measurement procedure, and setup can be found in [14] and [15].

III. *K*-Factor Estimation

For a nontime dispersive channel, equivalent to a nonfrequency selective channel, where there is a dominant

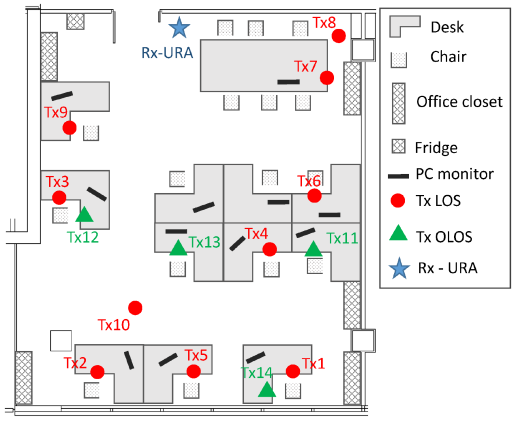

Fig. 1. Schematic of the propagation environment, with Tx and Rx positions.

contribution, the CIR can be written as [1]

$$h(t) = h_D + \sqrt{P_R} h_S(t) \tag{1}$$

where h_D indicates the complex amplitude of the dominant contribution, with a power equal to $P_D = |h_D|^2$, and $\sqrt{P_R} h_S(t)$ is a zero mean complex Gaussian process representing the stochastic MPCs (i.e., the reflected, diffracted, and scattered components) with a power $2\sqrt{P_R}$. Under these conditions, the envelope of $h(t)$ can be described by a Rice distribution [2], where the Rician *K*-factor is defined as

$$K \triangleq \frac{P_D}{2P_R}. \tag{2}$$

The value of the *K*-factor can be estimated using different estimators, such as the classical method of moments from the envelope of $h(t)$ [10].

In a wideband receiver, the MPCs can be distinguished by their propagation delay and the CIR can be expressed as [2]

$$h(t,\tau) = h_D \delta(\tau - \tau_0) + \sum_{m=1}^{M} \sqrt{P_{R,m}} h_{S,m}(t) \delta(\tau - \tau_m) \tag{3}$$

where $\sqrt{P_{R,m}} h_{S,m}(t)$ represents the sum of the M MPCs reaching the Rx antenna with a delay τ_m, h_D is the amplitude of the dominant contribution reaching the receiver with a delay τ_0, and $\delta(\cdot)$ is the Dirac function. Under the WSSUS assumption, the CIR can be written as

$$h(t,\tau) = h_D \delta(\tau - \tau_0) + \sum_{m=1}^{M} a_m e^{j2\pi f_{\max} \cos(\vartheta_m) t + \theta_m} \delta(\tau - \tau_m) \tag{4}$$

being a_m the amplitude, $f_{\max}$ the maximum Doppler frequency, ϑ_m the angle of arrival, and θ_m the phase associated to the mth stochastic MPC. From $h(t,\tau)$, the CTF of the wideband channel, denoted by $H(t,f)$, is [1]

$$H(t,f) = \int_{\tau} h(t,\tau) \exp(-j2\pi f \tau) d\tau \tag{5}$$

and therefore

$$H(t,f) = h_D e^{-j2\pi f\tau_0} + \sum_{m=1}^{M} a_m e^{j2\pi f_{\max}\cos(\vartheta_m)t+\theta_m-2\pi f\tau_m}. \quad (6)$$

If $H(t_0,f)$ represents the CTF at the instant t_0, the Rician *K*-factor can be calculated as

$$K = \frac{|h_D e^{-j2\pi f\tau_0}|^2}{|\sum_{m=1}^{M} a_m e^{j2\pi f_{\max}\cos(\vartheta_m)t_0+\theta_m-2\pi f\tau_m}|^2}. \quad (7)$$

Now, under the assumption of US in the delay variable [1], and taking into account the random nature of the complex amplitude and phase associated to the stochastic MPCs, and invoking the central limit theorem (CLT), (7) is reduced to [12]

$$K = \frac{|h_D|^2}{\sum_{m=1}^{M}|a_m|^2}. \quad (8)$$

In (8), the numerator indicates the power associated to the dominant contribution, and the denominator takes into account the power of the stochastic MPCs. In this way, as proposed in [12], the *K*-factor can be estimated from wideband channel measurements in the frequency domain. Thus, if $H(t_0,f_n)$ is the CTF for the *n*th frequency sample, the *K*-factor can be estimated using the method of moments as [10], [12]

$$\hat{K} = \frac{\sqrt{G_a^2 - G_v}}{G_a - \sqrt{G_a^2 - G_v}} \quad (9)$$

where

$$G_a = \frac{1}{N}\sum_{n=1}^{N}|H_n|^2 \quad (10)$$

$$G_v = \frac{1}{N-1}\left(\sum_{n=1}^{N}|H_n|^4 - NG_a^2\right) \quad (11)$$

being N the frequency samples of the CTF.

On the other hand, the power associated with the dominant contribution can be extracted from the PDP, denoted by $P(\tau)$. If $H(t_0,f)$ is the measured CTF at the instant t_0, the CIR of the wideband channel is given by [1]

$$h(t_0,\tau) = \int_f H(t_0,f)\exp(j2\pi f\tau)df \quad (12)$$

and under the WSSUS assumption, the PDP at the instant t_0 can be obtained as [1]

$$P(\tau) \equiv P(t_0,\tau) = E\{|h(t_0,\tau)|^2\}. \quad (13)$$

From the knowledge of $P(\tau)$, the *K*-factor can be estimated through the following expression:

$$\hat{K} = \frac{\sum_{l=1}^{L}\int_{\tau_l-\Delta\tau}^{\tau_l+\Delta\tau}P(\tau)d\tau}{\int_0^{\infty}P(\tau)d\tau - \sum_{l=1}^{L}\int_{\tau_l-\Delta\tau}^{\tau_l+\Delta\tau}P(\tau)d\tau} \quad (14)$$

where the numerator is an estimate of the power associated to the L dominant contributions, with τ_l the propagation delay of the lth dominant contribution, over an integration interval equal to $2\Delta\tau$. The denominator provides an estimate of the power associated with the remaining MPCs. The integration interval takes into account the windowing effect that occurs in the frequency domain when the CTF is measured by the VNA [16]. We have considered $\Delta\tau = 1/B_W$, being B_W the bandwidth of the CTF, which corresponds to the delay resolution in $P(\tau)$.

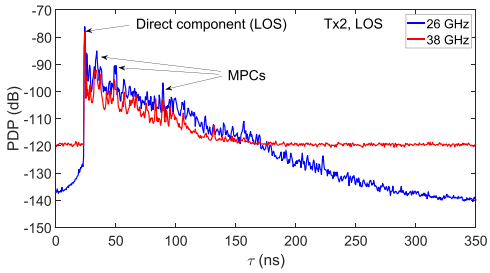

Fig. 2. PDP measured at 26 and 38 GHz at the Tx2 position in LOS.

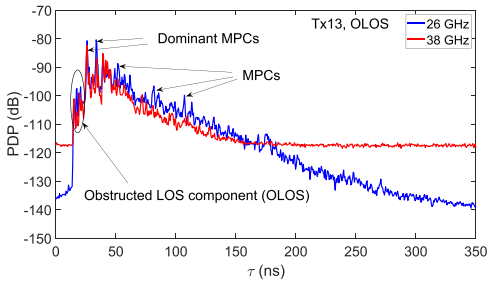

Fig. 3. PDP measured at 26 and 38 GHz at the Tx13 position in OLOS.

As an example, Figs. 2 and 3 show the measured PDP at 26 and 38 GHz in LOS and OLOS condition, respectively. There is a dominant contribution in LOS, which is the direct component, whereas in the OLOS, the absence of the LOS component causes other reflected MPCs to become dominant (two contributions in the PDP of Fig. 3).

IV. Results and Discussion

For each Tx antenna location, the value of the *K*-factor is estimated at each of the 144 (12×12) URA positions. The estimation is performed in frequency from the measured CTF using (9), and through the PDP using (14). A bandwidth of 2 GHz is considered in both methods. Thus, $\Delta\tau = 1/(2\,\text{GHz}) = 0.5$ ns in (14), and a power threshold level (TH) equal to 30 dB is considered in the PDP estimation. This value of TH corresponds to the case of minimum signal-to-noise ratio, which occurs at the maximum Tx–Rx distance and a the highest frequency band (38 GHz). Fig. 4 shows the cumulative distribution function (CDF) of the estimated *K* values, in logarithmic units, in the 26, 28, 33, and 38 GHz bands under LOS condition. Both estimation methods provide a very similar median value, particularly in the 26 and 28 GHz frequency bands. Fig. 5 shows the CDF of the *K*-factor in OLOS condition. In this case, dominant MPCs with an amplitude higher than 2 dB below the maximum of the PDP have been considered. The differences exhibited in the *K*-factor for low CDF values, in both LOS and OLOS, are mainly due

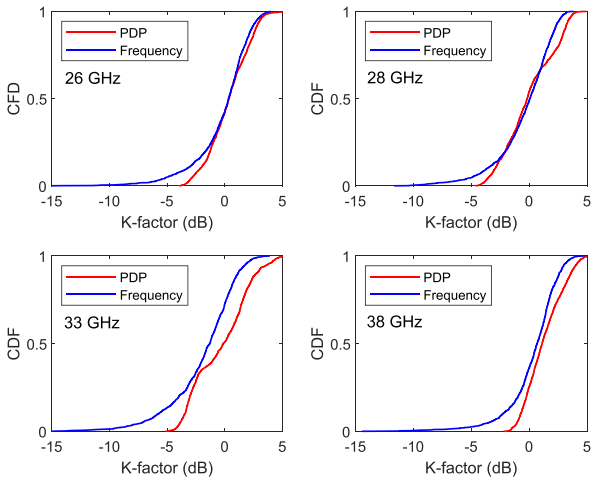

Fig. 4. CDF of the *K*-factor, in logarithmic units, for the 26, 28, 33 and 38 GHz frequency bands in LOS condition.

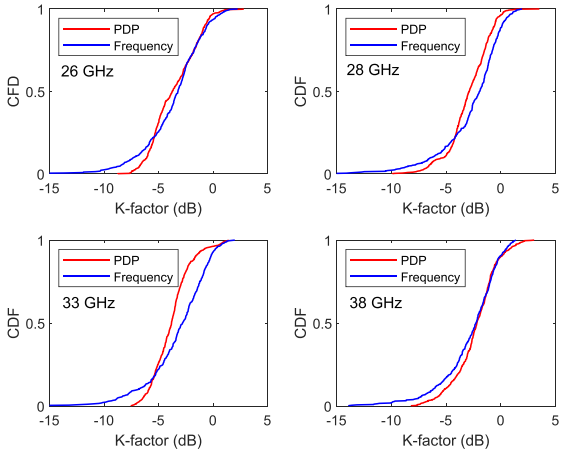

Fig. 5. CDF of the *K*-factor, in logarithmic units, for the 26, 28, 33 and 38 GHz frequency bands in OLOS condition.

TABLE I
K-FACTOR VALUES, IN LOGARITHMIC UNITS (DB): MEAN VALUE (STANDARD DEVIATION)

	26 GHz	28 GHz	33 GHz	38 GHz
LOS				
PDP	0,32 (1,79)	-0,01 (2,19)	-0.34 (2,44)	1,27 (1,60)
Frequency	-0,17 (2,42)	-0,39 (2,43)	-1,87 (2,83)	0,32 (2,19)
OLOS				
PDP	-3,54 (2,11)	-2,92 (1,91)	-3,79 (1,72)	-2,31 (1,97)
Frequency	-3,60 (2,72)	-2,61 (2,75)	-3,20 (2,74)	-2,78 (2,57)

to: 1) the power TH set in the PDP derivation, since when it increases the total power associated with the PDP is reduced, and as a result the value of K is overestimated; and 2) the value of $\Delta\tau$ involved in (14), since when it increases the value of K is also overestimated. The effect of these factors on the value of K requires further investigation, although their effect on the median value is minimal.

Table I summarizes the mean value (first-order sample moment) and the standard deviation (second-order sample moment), in logarithmic units, of the estimated K-factor. The differences in the mean value range from 0.38 to 1.53 dB under LOS, with a mean value of about 0.83 dB, while under OLOS the differences range from 0.06 to 0.59 dB, with a mean value close to 0.35 dB. The standard deviation values are higher when the K-factor is estimated from the CTF, although the differences are significantly less than 1 dB in most situations.

Since both methods provide very similar results, it is preferable to use the estimator based on the moment method given in (9), working directly with the measured CTF, especially in OLOS, where the identification of the dominant MPCs is more complicated. It should also be noted that when estimating the PDP it is necessary to properly set the value of the TH, which directly affects the estimation of the power associated with the stochastic contributions.

The values of the K-factor derived in this study are lower than those published in other works at mmWave frequencies for indoor environments [17], [18], [19], [20], [21]. In particular, a mean value of 9.04 dB was obtained in [17] at 26 GHz in a large office, and a mean value of 6.15 dB was derived in [18] at 28 GHz in an open office environment, both in LOS conditions. Our propagation scenario can be considered as a closed office environment, where the dimensions are smaller, resulting in a higher number of reflected contributions. As a result, the power associated with the stochastic MPCs increases, resulting in lower values of the K-factor. This behavior can be very well observed in Figs. 2 and 3, where the maximum propagation delay is high, with delay-spread values of the order of 15 and 20 ns in LOS and OLOS conditions, respectively. The results suggest that the K-factor is correlated with the dimensions of the propagation environment, decreasing as the dimensions are reduced.

Since the performance of MIMO systems improves as the stochastic MPCs increase [17], [22], corresponding to lower K-factor values, the results obtained here indicate that it is possible to employ massive MIMO techniques in order to increase the capacity of wireless systems in this type of scenario, even under LOS propagation condition.

V. CONCLUSION

In this letter, the K-factor has been estimated in a typical office scenario from wideband channel measurements. The method of moments and the PDP-based method have been used. The K-factor values have been particularized to the potential 26, 28, 33, and 38 GHz frequency bands for the deployment of the future wireless networks. The results show that both methods provide similar average values, making them suitable for evaluating the channel selectivity from experimental measurements. However, it is more appropriate to estimate the K-factor directly from the samples of the measured CTF using the method of moments. The effect of $\Delta\tau$ and the power TH parameters on the K-factor estimation when the PDP-based method is used requires further investigation in order to establish a direct comparison between the two methods, and will be addressed as a future research.

The results derived from this work are interesting for the design, performance evaluation, and deployment of wireless systems in indoor office scenarios operating at mmWave frequencies.

REFERENCES

[1] J. D. Parsons, *The Mobile Radio Propagation Channel*, 2nd ed. Hoboken, NJ, USA: Wiley, 2000.

[2] A. F. Molisch, *Wireless Communications*, 2nd ed. Hoboken, NJ, USA: Wiley-IEEE Press, 2010.

[3] D. Greenwood and L. Hanzo, "Characterization of mobile radio channels," in *Mobile Radio Communications*, R. Steele and L. Hanzo, Ed., 2nd ed. Hoboken, NJ, USA: Wiley, 1999.

[4] A. A. Abu-Dayya and N. C. Beaulieu, "Microdiversity on Rician fading channels," *IEEE Trans. Commun.*, vol. 42, no. 6, pp. 2258–2267, Jun. 1994.

[5] M. A. Al-Jarrah, K.-H. Park, A. Al-Dweik, and M.-S. Alouini, "Error rate analysis of amplitude-coherent detection over Rician fading channels with receiver diversity," *IEEE Trans. Wireless Commun.*, vol. 19, no. 1, pp. 134–147, Jan. 2020.

[6] K. Raghunath, Y. U. Itankar, A. Chockalingam, and R. K. Mallik, "BER analysis of uplink OFDMA in the presence of carrier frequency and timing offsets on Rician fading channels," *IEEE Trans. Veh. Technol.*, vol. 60, no. 9, pp. 4392–4402, Nov. 2011.

[7] Y. Hu, Y. Hong, and J. Evans, "Angle-of-arrival-dependent interference modeling in Rician massive MIMO," *IEEE Trans. Veh. Technol.*, vol. 66, no. 7, pp. 6171–6183, Jul. 2017.

[8] O. Özdogan, E. Björnson, and E. G. Larsson, "Massive MIMO with spatially correlated Rician fading channels," *IEEE Trans. Commun.*, vol. 67, no. 5, pp. 3234–3250, May 2019.

[9] K. K. Talukdar and W. D. Lawing, "Estimation of the parameters of the Rice distribution," *J. Acoust. Soc. America*, vol. 89, no. 3, pp. 1193–1197, 1991.

[10] L. Greenstein, D. Michelson, and V. Erceg, "Moment-method estimation of the Ricean K-factor," *IEEE Commun. Lett.*, vol. 3, no. 6, pp. 175–176, Jun. 1999.

[11] K. E. Baddour and T. J. Willink, "Improved estimation of the Ricean K-factor from I/Q fading channel samples," *IEEE Trans. Wireless Commun.*, vol. 7, no. 12, pp. 5051–5057, Dec. 2008.

[12] P. Tang, J. Zhang, A. F. Molisch, P. J. Smith, M. Shafi, and L. Tian, "Estimation of the K-factor for temporal fading from single-snapshot wideband measurements," *IEEE Trans. Veh. Technol.*, vol. 68, no. 1, pp. 49–63, Jan. 2019.

[13] World Radiocommunications Conference, Resolutions COM4/8-9, 2019.

[14] L. Rubio et al., "Millimeter-wave channel measurements and path loss characterization in a typical indoor office environment," *Electronics*, vol. 12, no. 4, pp. 844–860, 2023.

[15] L. Rubio et al., "Millimeter wave channel measurements in an intra-wagon environment," *IEEE Trans. Veh. Technol.*, vol. 68, no. 12, pp. 12427–12431, Dec. 2019.

[16] T. Dammes, W. Endemann, and R. Kays, "Frequency domain channel measurements for wireless localization - Practical considerations and effects of the measurement," in *Proc. 18th Eur. Wireless Conf.*, 2012 pp. 1–8.

[17] Q. Wang, S. Li, X. Zhao, M. Wang, and S. Sun, "Wideband millimeter-wave channel characterization based on LOS measurements in an open office at 26 GHz," in *Proc. IEEE 83rd Veh. Technol. Conf.*, 2016, pp. 1–5.

[18] P. Tang, J. Zhang, M. Shafi, P. A. Dmochwski, and P. J. Smith, "Millimeter wave channel measurements and modelling in an indoor hotspot scenario at 28 GHz," in *Proc. 88th Veh. Technol. Conf.*, 2018, pp. 1–5.

[19] S. Li, Y. Liu, L. Lin, X. Sun, S. Yang, and D. Sun, "Millimeter-wave channel simulation and statistical channel model in the cross-corridor environment at 28 GHz for 5G wireless system," in *Proc. Int. Conf. Microw. Millimeter Wave Technol.*, 2018, pp. 1–3.

[20] Y. Guan, J. Zhang, L. Tian, P. Tang, and T. Jiang, "A comparative study for indoor factory environments at 4.9 and 28 GHz," in *Proc. 14th Eur. Conf. Antennas Propag.*, 2020, pp. 1–5.

[21] X. Zhang, G. Qiu, J. Zhang, L. Tian, P. Tang, and T. Jiang, "Analysis of millimeter-wave channel characteristics based on channel measurements in indoor environments at 39 GHz," in *Proc. 11th Int. Conf. Wireless Commun. Signal Process.*, 2019, pp. 1–6.

[22] G. Taricco and E. Riegler, "On the ergodic capacity of correlated Rician fading MIMO channels with interference," *IEEE Trans. Inf. Theory*, vol. 57, no. 7, pp. 4123–4137, Jul. 2011.